

Pilotless FS-FBMC for Flexible Spectrum Access and Sharing

Tien Vo-Huu
Northeastern University
tienvh@ccs.neu.edu

Norbert Ludant
Northeastern University
ludant.n@northeastern.edu

Triet Vo-Huu
Northeastern University
vohuudtr@ccs.neu.edu

Guevara Noubir
Northeastern University
g.noubir@northeastern.edu

Abstract—The RF spectrum is increasingly congested. Filter Bank Multicarrier (FBMC) is a promising technology for fine-grained spectrum sharing and exploiting the pockets left by co-existing heterogeneous technologies. However, the use of FBMC is hindered by the lack of techniques to support its potential for flexibility and agility. We introduce a spectrum-flexible design for Frequency Spreading Filter Bank Multicarrier (FS-FBMC). The key novelty of our approach, to achieve practical flexibility, is that it does not require pilot subcarriers for its operation. Therefore it can operate over narrow pockets of spectrum as well as wider bands without the need to restructure the physical layer. This gain in agility and spectral efficiency, requires the design of new channel estimation and equalization algorithms, as virtually all existing FBMC (and OFDM) systems rely on pilot subcarriers. We introduce a novel pilotless iterative channel equalization algorithm for FS-FBMC. We implement and extensively evaluate our approach. We demonstrate its robustness, and spectral efficiency. For instance, relatively to (Wi-Fi) OFDM the pilotless feature of our system and absence of Cyclic Prefix results in 46% better spectral efficiency. We also demonstrate that our system is flexible and can scale from 156 kHz to 16 MHz, therefore able to fit in most spectrum pockets. Our system was a finalist in the DARPA Spectrum Collaboration Challenge (SC2) in 2019 (and the base of our winning team in 2017 and 2018).

I. INTRODUCTION

Wireless communications revolutionized nearly every aspects of human life, from e-learning, economy and industry to social interactions. Many wireless technologies have been deployed to address the increasing communications and bandwidth demands of such services. Although each specific technology and standard offers different physical layer configurations and resource usages, all wireless technologies share the same scarce resource, the radio-frequency spectrum. Moreover, the different configurations at the physical layer create a highly heterogeneous ecosystem which does not use the spectrum in an optimal efficient way. As an example, we conducted a measurements campaign of the 2.4GHz band in several neighborhoods of Boston (USA), and identified the existence of various relatively small pockets of unused spectrum. These pockets, illustrated in Figure 1, change over time and space. In recent years, to improve the overall capacity of the channel, cognitive radios and other dynamic spectral sharing and allocation techniques gained considerable attention [1]–[4]. Previous research indicates that spectrum sharing can improve the overall capacity, but they also need to be carefully designed. For instance, transmissions from other deployed systems should not suffer from interference. Thus,

any proposed solution needs to limit interference to adjacent transmissions at the same time it is flexible.

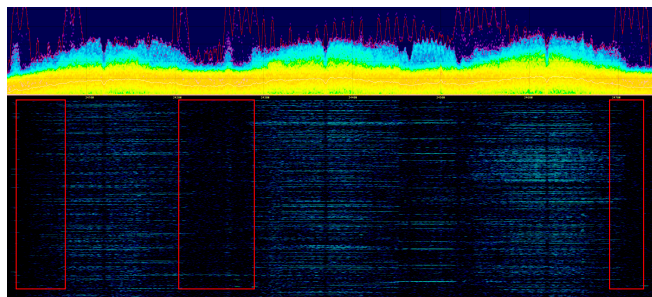


Fig. 1: Measurements campaign of the 2.4 GHz band in Boston (USA) reveals the existence of unused spectrum.

Orthogonal Frequency Division Multiplexing (OFDM) with Cyclic Prefix (CP) is currently the most widely employed waveform in multicarrier systems. This is due to its resilience against multipath and phase noise, and low complexity (e.g., Frequency Domain Equalization). However, CP-OFDM is not a good fit for dynamic spectrum sharing. This is due to the significant side-lobes (out-of-band) characteristic of OFDM, which creates high interference to adjacent transmissions, requiring a large number of guard subcarriers to reduce the out of band emissions. Filter Bank Multicarrier (FBMC) techniques are a promising alternative. They provide superior throughput thanks to the omission of cyclic prefix and guard bands, low out-of-band interference due to the use of narrow filters, and flexibility. A spectral comparison can be found in Figure 2, where the spectral containment properties of FBMC clearly outperform OFDM's, leaking little to none out-of-band emissions. Multiple realizations of FBMC have been presented in the literature, e.g., FBMC-QAM, FBMC-OQAM, each providing different complexities and characteristics. For instance, FBMC-OQAM can be realized by Polyphase Network or Frequency Spreading implementation. However, existing solutions are difficult to use in practice as the need for pilots limits the flexibility in exploiting arbitrary pockets of spectrum.

In this paper we introduce a novel pilotless FS-FBMC approach which provides spectral, design, and implementation flexibility, low interference, and high spectral efficiency. In order to take the flexibility of FS-FBMC one step further,

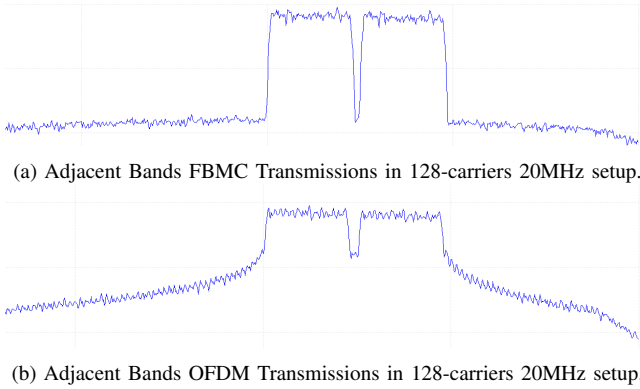


Fig. 2: Out of band emission comparison of FBMC and OFDM.

our design *does not rely on pilots*, as pilots constrain the flexibility of both the spectrum and the design. Thus, we develop a novel channel estimation technique that exploits the data constellation error to equalize the channel iteratively. We implement and extensively evaluate our design over different channels and modulations. Our results show that the design is able to achieve a BER of 1×10^{-6} at 15 dB SNR for 16-QAM modulation. Moreover, the lack of pilots along with the omission of a cyclic prefix increase the spectral efficiency of our system compared to the CP-OFDM (Wi-Fi) approach by 46% for the modulation and coding scheme 16-QAM 1/2.

Our results indicate that FBMC is a promising waveform for fine-grained spectrum sharing and its limitations can be addressed with our pilotless technique. We implemented our techniques and compared to Wi-Fi but also developed a full networking stack on top of it. This was the basis of our team (Sprite) solution in the Spectrum Collaboration Challenge (SC2) organized by DARPA [5]. Sprite was a winning team in 2017, 2018 and a finalist in 2019. We note that given the computational demands of the machine learning techniques required by the SC2 competition, the physical layer needed to be computationally efficient and robust. Our main contributions are as follows:

- We introduce a novel design for a pilotless FS-FBMC communication system, and develop a channel estimation and equalization technique that does not require pilots. Instead, it iteratively equalizes the channel exploiting the relative constellation error.
- We implement our design for SDR platforms and evaluate the performance both through a simulated, emulated and over the air channels.
- We demonstrate that our techniques and implementation are highly flexible operating seamlessly from 156 kHz to 16 MHz, and robust achieving a BER of 1×10^{-6} at 15 dB SNR for 16-QAM modulation.
- In addition to flexibility, the absence of cyclic prefix and pilots in our design leads to over 46% better spectral efficiency than Wi-Fi CP-OFDM.

The paper is structured as follows, in Section II, specific details about FS-FBMC are introduced, along with a descrip-

tion of channel equalization for FBMC. Our improved flexible design is discussed in Section III, focusing on the proposed novel pilotless channel estimation and equalization algorithm. The performance evaluation results of our system for different bandwidths and modulations are presented in Section IV. To conclude, Section V summarizes the implications of the proposed design and use cases.

II. BACKGROUND ON FILTER BANK MULTICARRIER

In this section we describe the relevant details of FBMC systems and its operation that will aid in the understanding of our proposed design and implementation.

FBMC as an evolution of OFDM. Initial research on filter bank based multicarrier systems started during the 1960s [6], [7]. Filter Bank Multicarrier divides the frequency spectrum in multiple narrow sub-channels, shaped by a set of carefully designed filters. Despite FBMC's potential, the added signal processing complexity initially hindered its adoption, and CP-OFDM is currently the most widely deployed multicarrier system. One of the benefits of OFDM is its low complexity of implementation due to the use of IFFT/FFT as synthesis (transmitter) and analysis (receiver) filters respectively. However, the use of FFT as a modulator creates multiple drawbacks, such as poor spectral power containment and the requirement of a guard time to ensure correct demodulation. FBMC overcomes these shortcomings by using a different choice of shaping filters. Whereas the filters used for OFDM use a rectangular pulse approach, FBMC shapes each subcarrier by what is termed a prototype filter. The prototype filter choice is an important design decision as it improves the time-frequency localization and has been widely investigated in the literature [8]. For instance, the use of different filters reduces the out-of-band emissions, and relaxes the synchronization requirements, for multi-user access, specially important for cognitive radio and fragmented spectrum [9]. Furthermore, FBMC does not require to append a Cyclic Prefix to each symbol as in OFDM to guarantee orthogonality, which implies a loss in spectral efficiency of up to 25%. This fact, along with FBMC not requiring guard periods further increases the spectral efficiency of FBMC systems. In-depth comparisons of OFDM and FBMC have been discussed in the literature, analyzing spectral differences, design considerations and their fit in systems with different requirements [10], [11].

OQAM as a modulation for FBMC. Filter Bank Multicarrier is a generalized approach and can operate for different modulations, both real and complex, such as PAM or QAM [6], [7]. However, the fact that neighboring sub-channels overlap in frequency domain renders the use of given modulations sub-optimal as commonly an empty sub-channel needs to be placed between two data sub-channels to avoid overlap and self-interference. If full rate is to be achieved by using all sub-channels, the modulation needs to be chosen carefully. In this way, it has been identified that Offset QAM (OQAM) is an ideal fit for FBMC communications to achieve higher throughputs as it can effectively use all set of sub-channels while

minimizes self-interference [12]. FBMC-OQAM separates real and imaginary parts such that they are transmitted alternatively as real symbols in consecutive sub-channels, satisfying the orthogonality constraint for neighboring channels [13]. FBMC-OQAM is an interesting option due to its increased spectral efficiency capabilities, although presents a number of challenges, such as intrinsic interference [14], [15].

Efficient FBMC implementations. One of the main drawbacks of FBMC is the increased signal processing in comparison to OFDM. Considerable efforts have been made in the research community to reduce the complexity of FBMC since early stages [16], [17]. Furthermore, numerous projects have been carried out in recent years to stimulate the research in FBMC and explore its capabilities for next generation wireless systems, such as PHYDYAS [18] and METIS [19]. Currently, there are two main approaches for efficient implementations of FBMC-OQAM: PolyPhase Network FBMC (PPN-FBMC) [13], and Frequency Spreading FBMC (FS-FBMC) [20], [21]. An advantage of FS-FBMC over PPN-FBMC is that channel equalization is performed in the frequency domain instead of time domain with no delay. One of the main concerns of FS-FBMC is the increase in computational complexity by the use of K -times larger FFT size (K is the overlapping factor often set to 4 in practice), schemes to reduce complexity have been proposed, finding that certain hardware implementations are more efficient than its PPN counterpart [17], [22].

Channel estimation and equalization in FBMC systems. The use of OQAM modulation carries certain implications at the receiver side. Although the interference is reduced for neighboring channels due to the orthogonality of OQAM systems, the orthogonality is only in the real domain, and an imaginary component remains, generating interference. This intrinsic interference needs to be cancelled in order to use a scattered pilot-based channel estimation method for OQAM, increasing complexity [23], [24]. Multiple pilot schemes have been proposed, such as preamble-based [25], and mostly scattered-pilot approaches [26]–[28]. However, most approaches consider an FBMC-OQAM system with a PPN implementation, which does not reflect the peculiarities of channel estimation for FS-FBMC systems. For FS-FBMC, the pilots are placed in the normal frequency domain, however, the channel effect is in the extended-FFT domain, and pilots are retrieved after de-spreading at the receiver. Papers explore an iterative approach to this issue for FS-FBMC [29].

The design of our Pilotless FS-FBMC addresses these challenges and peculiarities, maintaining the benefits of FBMC, and leading to spectrum-flexible robust algorithms and a practical system.

III. FLEXIBLE PILOTLESS FS-FBMC DESIGN

In this section, we introduce our Frequency Spreading (FS) FBMC design and describe the physical layer choices that enable increased flexibility. In particular, we present a novel FBMC pilotless channel estimation and equalization technique.

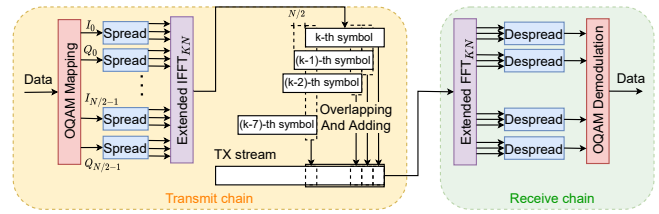


Fig. 3: FS-FBMC transmitting and receiving loopback with overlapping factor $K = 4$ and FFT size N .

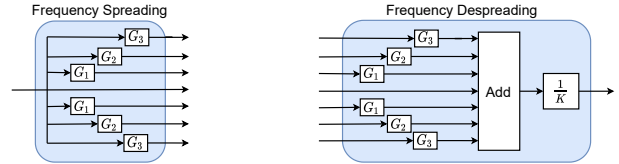


Fig. 4: Frequency spreading and despreading.

A. Flexible FS-FBMC Design Overview

Base Design. Our design approach extends previous work on FS-FBMC [20] with the goal of optimizing and increasing the flexibility of the system. Figure 3 depicts the high-level design of a basic FS-FBMC transmitting and receiving loopback, where the FBMC signal is transmitted over a noise-free channel (for illustration purpose).

At the transmitter, the data is modulated according to Offset QAM (OQAM) rules to maintain the orthogonality of FBMC subcarriers. The complex I and Q components are then separately spread into KN values and fed to an extended IFFT module with size KN . This approach, in comparison to PPN-FBMC with N subcarriers, is viewed as upsampling the signal by K times and applying a frequency-domain filter on the data points. In this work, we use $K = 4$, which is the overlapping factor indicating the number of overlapped subcarriers between two real data points. Each FBMC symbol produced by the extended IFFT consists of KN samples, which are then shifted by $N/2$ samples and added altogether to previous FBMC symbols to create the overlapped signal in the time domain for transmission.

At the receiver, a chunk of KN samples from the received stream is fed to the extended FFT module to obtain the FBMC symbol, whose complex I and Q components are independently despread before an OQAM demodulation process can be performed to retrieve the original data. It is emphasized that while each received chunk is the result of the overlapping and adding of multiple shifted FBMC symbols in the time domain, the Inter-Symbol Interference (ISI) is eliminated due to the OQAM mapping, allowing the removal of cyclic prefix and increasing the bandwidth efficiency in comparison to OFDM (e.g., cyclic prefix results in 25% overhead in Wi-Fi).

FS-FBMC intrinsic flexibility. For the spreading filter (Figure 4), we use the following real tap values: $G_1 = 0.971960$, $G_2 = 0.707107$, $G_3 = 0.235147$. This filter ensures that interference from non-adjacent subcarriers is lower than -60 dB, which implies two *independent* (e.g., two non-synchronized

users) FBMC transmissions can be carried out with negligible Inter-Carrier Interference (ICI) even if channel spacing is only one subcarrier [20]. Thanks to the good spectral localization of FBMC, our system can carry transmissions with high flexibility such that it can fit into spectrum pocket without creating interference to adjacent bands. In contrast, OFDM requires guard bands to minimize ICI (e.g., Wi-Fi guard band costs 25% of its operating channel). It is worth noting that our system's flexibility is achieved by simply changing the location and number of subcarriers without reconfiguring the RF center frequency and sample rate, and as a result, it incurs zero latency.

Going pilotless to achieve real flexibility. In contrast with traditional designs using pilots to estimate the effects of the channel, our system does not require these known data for channel estimation and equalization. Pilots constrain the flexibility in the design and operation of systems, such as requiring manual and careful design for different number of subcarriers in the system, or for operating in different environments (e.g., cellular, Wi-Fi, vehicular networks). Our system avoids the use of pilots, therefore the receiver requires less prior knowledge of the system, making it flexible from the design viewpoint. This unleashes the capabilities of FS-FBMC of seamlessly operating at different bandwidths and to achieve higher throughput by using all subcarriers for data.

B. Pilotless Channel Estimation and Equalization Technique

In order to develop a flexible design that does not require the knowledge of pilot values, our channel estimation and equalization have to rely on other signal properties that reflect the channel evolving. To tackle this problem, we look into the data itself and use it to correct the channel. This approach is known as decision-directed equalization, where the data deviation from the constellation points can be used to estimate the channel state information (CSI). While this technique has been extensively studied for OFDM [30]–[32], extending it to our system requires a FS-FBMC-specific solution to resolve the non-linearity relation between the original frequency domain, where the data is constructed, and the extended frequency domain, where the channel effect needs to be equalized.

1) *Channel Effect and Estimation:* This subsection provides a mathematical description of the channel impact on the data symbols in our FS-FBMC system. We first establish an approximation for the channel and propose a novel lookup table based method for refining the estimation. Our approach uses the data symbols for channel estimation, leading to the pilotless design.

System Model. We start the discussion by first presenting the FS-FBMC/OQAM process with the main operations taking place at the transmitter and receiver sides. For the sake of simplicity, it is assumed that we are transmitting data on the whole operational channel, i.e., utilizing all N subcarriers to convey data. In practice, especially for spectrum pocket, only a subset of subcarriers will carry information while the rest is filled with zeros.

In our system (Figure 3), the data synthesis (on the transmitter side) is taking place for every chunk of $N/2$ constellation complex symbols modulated from the input binary data. Consider the m -th chunk to be transmitted, let $d_{m,n} = i_{m,n} + jq_{m,n}$ denote the n -th constellation point with $i_{m,n}$ and $q_{m,n}$ being the in-phase and quadrature-phase components of $d_{m,n}$. The spreading of I and Q components, implemented based on a filter $\mathbf{g} = [g_0 \dots g_{2K-1}] = [G_1, G_2, G_3, 1, G_3, G_2, G_1, 0]$ as in Figure 4, produces two sequences:

$$\begin{aligned} \mathbf{I}_m &= [I_{m,0} \dots I_{m,KN-1}], & I_{m,2Kn+k} &= g_k i_{m,n}, \\ \mathbf{Q}_m &= [Q_{m,0}, \dots, Q_{m,KN-1}], & Q_{m,2Kn+k} &= g_k q_{m,n}. \end{aligned} \quad (1)$$

The input of the extended IFFT module is formed by shifting \mathbf{Q}_m by K and, depending on the parity of the chunk index m , alternatively feeding \mathbf{I}_m and \mathbf{Q}_m to the real and imaginary parts of the IFFT input $\mathbf{X}_m = [X_{m,0} \dots X_{m,KN-1}]$. This mapping is expressed as

$$X_{m,l} = I_{m,l}\gamma_0 + Q_{m,l-K}\gamma_1, \quad l = 0 \dots KN - 1, \quad (2)$$

where $\gamma_0 = j^{m \bmod 2}$ and $\gamma_1 = j^{(m+1) \bmod 2}$. For concise discussion, we assume the current FBMC symbol index m is an even number, therefore $\gamma_0 = 1$ and $\gamma_1 = j$. This assumption is used to establish the mathematical relations in the rest of this section.

On the receiver side, if we define $\omega_{m,l}$ as the intrinsic interference from neighboring symbols, the FFT module produces $\hat{\mathbf{X}}_m = [\hat{X}_{m,0}, \dots, \hat{X}_{m,KN-1}]$, which is the sum of the original FBMC symbol and the intrinsic interference: $\hat{X}_{m,l} = X_{m,l} + \omega_{m,l}$. For convenience, we use the notation $\Re(\mathbf{X}_l)$ and $\Im(\mathbf{X}_l)$ to represent the real and imaginary sub-vectors of \mathbf{X} , starting from index l and consisting of $2K$ elements. Specifically, $\Re(\mathbf{X}_l) = [Re(X_l), \dots, Re(X_{l+2K-1})]$ and $\Im(\mathbf{X}_l) = [Im(X_l), \dots, Im(X_{l+2K-1})]$.

To recover the original data $d_{m,n}$ from the received FBMC symbol $\hat{\mathbf{X}}_m$, we perform the despreading process, represented by the dot product, as follows.

$$\begin{aligned} \hat{d}_{m,n} &= \mathbf{g} \cdot \Re(\hat{\mathbf{X}}_{m,nK}) + j \cdot \mathbf{g} \cdot \Im(\hat{\mathbf{X}}_{m,nK-K}) \\ &= d_{m,n} + \underbrace{\mathbf{g} \cdot (\Re(\omega_{m,nK}) + j\Im(\omega_{m,nK-K}))}_{\Omega_{m,n}=0}. \end{aligned} \quad (3)$$

Thanks to the good localization of FBMC, despreading $\hat{\mathbf{X}}_m$ can eliminate the intrinsic interference $\Omega_{m,n}$ and recover $d_{m,n}$.

Channel Effect. Now consider the transmitted signal is affected by the channel during the propagation, the m -th received FBMC symbol in the extended frequency domain becomes $\tilde{X}_{m,l} = H_{m,l}(X_{m,l} + \omega_{m,l})$ with $H_{m,l}$ indicating the channel in the l -th subcarrier of the extended frequency domain within the duration of the m -th FBMC symbol. In many realistic environments, the channel can vary slowly between subcarriers and across multiple FBMC symbols. In this work, we consider such a slow-fading channel, where $H_{m+\Delta,nK+\Delta} = Ce^{j\alpha}$ with amplitude C and angle α remain constant for $-K \leq \Delta \leq K$. The channel effect on the received

symbols is described in the following equation.

$$\begin{aligned} \Re(\tilde{\mathbf{X}}_{m,nK}) &= C \cos \alpha \Re(\hat{\mathbf{X}}_{m,nK}) - C \sin \alpha \Im(\hat{\mathbf{X}}_{m,nK}) \\ \Im(\tilde{\mathbf{X}}_{m,nK-K}) &= C \cos \alpha \Im(\hat{\mathbf{X}}_{m,nK-K}) + C \sin \alpha \Re(\hat{\mathbf{X}}_{m,nK-K}). \end{aligned} \quad (4)$$

If (we will release this assumption later on) the channel variation is small enough, we can assume $\sin \alpha \approx 0$, then based on Equation (4), we can achieve the following approximation:

$$\begin{aligned} \Re(\tilde{\mathbf{X}}_{m,nK}) &= C \cos \alpha \Re(\hat{\mathbf{X}}_{m,nK}) \\ \Im(\tilde{\mathbf{X}}_{m,nK-K}) &= C \cos \alpha \Im(\hat{\mathbf{X}}_{m,nK-K}) \end{aligned} \quad (5)$$

Applying the despreading process on Equation (5) gives the channel impact on the data symbol $d_{m,n}$.

$$\tilde{d}_{m,n} = \mathbf{g} \Re(\tilde{\mathbf{X}}_{m,nK}) + j \mathbf{g} \Im(\tilde{\mathbf{X}}_{m,nK-K}) = d_{m,n} C \cos \alpha. \quad (6)$$

Channel Estimation. The result in Equation (6) suggests that the channel could be estimated as follows.

$$C = \left| \frac{\tilde{d}_{m,n}}{d_{m,n}} \right|, \quad \alpha = \pm \arccos \frac{\tilde{d}_{m,n}}{d_{m,n} C}. \quad (7)$$

However, two issues arise: (1) $d_{m,n}$ is not known, and (2) cosine is a symmetric function, as a result we would obtain an ambiguous channel phase. Our approach to the first issue is based on the intuition and experimental results that if the signal-to-noise ratio (SNR) is reasonable, $\tilde{d}_{m,n}$ and $d_{m,n}$ are in close proximity with high confidence, while a low SNR would conversely result in high decoding errors even if the channel is perfectly estimated. Therefore, by guessing $d_{m,n}$ as the closest constellation point to $\tilde{d}_{m,n}$, the channel estimation can be handled via Equation (7). For the second issue, since the derived phase can be positive and negative values, to find the correct one, we use the following selection method, in which we evaluate the total constellation errors in the FBMC symbols for each phase value, and choose the value corresponding to the better accuracy. Full description of this approach is described in Section III-B2.

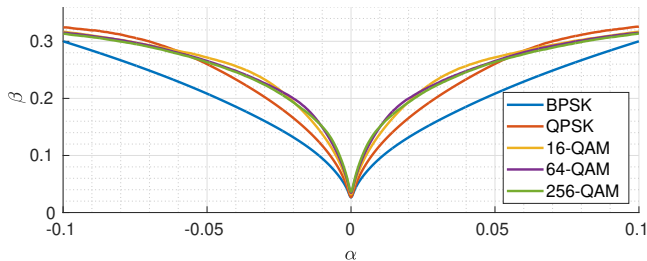


Fig. 5: Nonlinear relation between channel phase α and data symbol deviation β suggests an iterative approach for channel estimation to resolve the ambiguity.

Fine-grained Estimation. Recall that the established Equation (6) is based on the assumption of the channel phase α being sufficiently small. When α is large, the estimate using Equation (7) becomes less accurate. To improve the accuracy,

we revisit Equation (4) and apply the despreading operation:

$$\tilde{d}_{m,n} = \mathbf{g} \Re(\tilde{\mathbf{X}}_{m,nK}) + j \mathbf{g} \Im(\tilde{\mathbf{X}}_{m,nK-K}) \quad (8)$$

$$= d_{m,n} C \cos \alpha + j C \sin \alpha \cdot \mathbf{g} (\Re(\tilde{\mathbf{X}}_{m,nK-K}) + j \Im(\tilde{\mathbf{X}}_{m,nK})). \quad (9)$$

The second term in Equation (9) is the combination of the channel effect and interference from adjacent subcarriers and nearby FBMC symbols. To find α , we first take the real part on both sides of Equation (9) and obtain

$$\text{Re}(\tilde{d}_{m,n}) = \text{Re}(d_{m,n}) C \cos \alpha - \text{Im}(d_{m,n-1}) C \sin \alpha. \quad (10)$$

Let us define a function $f(\alpha)$ and a pseudo variable β as follows.

$$f(\alpha) = \arccos \left(\cos \alpha - \frac{\text{Im}(d_{m,n-1})}{\text{Re}(d_{m,n})} \sin \alpha \right) \quad (11)$$

$$\beta = \arccos \left(\frac{\text{Re}(\tilde{d}_{m,n})}{C \text{Re}(d_{m,n})} \right). \quad (12)$$

Based on Equations (10) to (12), we have $\beta = f(\alpha)$. Intuitively, β is the measure of how far the received despread data symbol $\tilde{d}_{m,n}$ deviates from its closest constellation point $d_{m,n}$, whereas $f(\alpha)$ describes the relation between α and β . To remove the dependence on data symbols in $f(\alpha)$, we use an empirical approach, in which the channel is simulated by changing α in fine-grained steps within a range $[-\alpha_0, \alpha_0]$, and by running transmission of random data packets, the deviation β is computed and recorded into a lookup table. It is worth emphasizing that since our FS-FBMC receiver performs the initial channel estimation using packet preambles and adaptively updates the channel during the packet payload reception, the channel phase change (relative to the previous value) is generally within a small range. Specifically we use $\alpha_0 = 0.1$ determined based on real testbed evaluation. Figure 5 shows the relation between α and β for various modulation schemes when simulating on random data. It is clearly observed that $f(\alpha)$ is an even function and modulation dependent. Accordingly, for each observed value of β there are two possible values for the channel phase: $\alpha = \pm f^{-1}(\beta)$. To resolve this ambiguity, we use an iterative approach as described in Section III-B2.

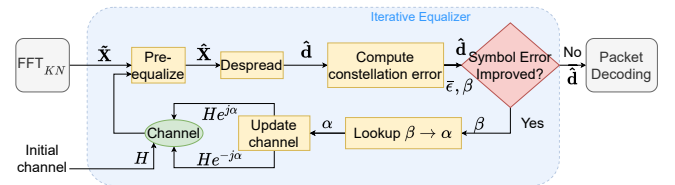


Fig. 6: Pilotless Channel Estimation and Equalization Block Diagram.

2) *Pilotless Iterative Equalization Algorithm:* The main idea of our pilotless equalization approach is to iteratively fine-tune the channel estimation until the overall constellation error falls below a threshold or is not reduced anymore. Each iteration, depicted in Figure 6, involves the FBMC despreading, constellation demodulating, error computation,

and channel update. The algorithm for pilotless iterative equalization, illustrated in Algorithm 1, is performed on FBMC symbol basis.

Pre-equalization. Each received FBMC symbol is pre-equalized with the previous channel estimation \mathbf{H} , obtained during the processing of the previous symbol, to achieve $\tilde{\mathbf{X}} = \tilde{\mathbf{X}}/\mathbf{H}$. For the first FBMC symbol of packet, the initial channel is computed based on the preamble from the frame synchronization stage (which is not in the scope of this paper).

Despreading and Computing Constellation Error. Next, we obtain the data symbols $\tilde{\mathbf{d}}$ by despreading $\tilde{\mathbf{X}}$ based on Equation (8). Demodulating $\tilde{\mathbf{d}}$ gives us the binary sequence that is ready for packet decoding to retrieve the original message. During the demodulation process, the closest constellation points are revealed and used to compute the deviation β according to Equation (12). In addition, the constellation error ϵ is also computed based on the distance between the received data symbols $\tilde{\mathbf{d}}$ and their closest points \mathbf{d} on the constellation mapping. We note that while our system supports dynamic modulation schemes, the knowledge of constellation mapping is known to the receiver at the time of equalization. For the packet header, the modulation is fixed and known in advance. For the packet payload, the modulation is available via the header information. The constellation error is given by

$$\epsilon = \frac{\sum_{n=0}^{N-1} (|\tilde{d}_{m,n} - d_{m,n}|)}{N}. \quad (13)$$

Now if the error ϵ falls below a good threshold ϵ_{good} , the channel estimate is believed to be accurate enough and the iterative equalization loop is complete for the current FBMC symbol. In practice, we choose ϵ_{good} to be one-fifth of the minimum distance in the constellation. For error larger than the good threshold, we iteratively perform channel updating as described in the following.

Channel Updating. Our channel updating is performed recursively, where each iteration consists of two main steps.

First, a new estimation for the channel is obtained by looking up β , computed from Equation (12), in the pre-built lookup table. For each value of β , we have two possibilities for the channel phase: $\alpha = f^{-1}(\beta)$ or $\alpha = -f^{-1}(\beta)$. The selection of correct value is determined based on the constellation error associated with each choice. This justification is done by two recursive calls to the equalization process itself, one with $\mathbf{H}' = \mathbf{H}e^{j\alpha}$ as the new initial channel, and another with $\mathbf{H}' = \mathbf{H}e^{-j\alpha}$.

Next, when the recursive call returns the estimate α' with an associated constellation error ϵ' , we compare and select the value of α' that corresponds to the lower error. We also check that the estimation is on the convergence by verifying the condition $\epsilon < \epsilon_{last}$, where ϵ_{last} is the error obtained in the last iteration. Intuitively this condition holds if we have progressive improvement on the estimation, otherwise the current iteration is terminated. Once the equalization is finished, the processing flow is continued with the packet decoding, and the current channel is stored to be used as the initial channel for the next

FBMC symbol equalization.

Algorithm 1 Pilotless Iterative Equalization

```

EQUALIZE( $\tilde{\mathbf{X}}, \mathbf{H}, \epsilon_{last}$ )
1   $\tilde{\mathbf{d}} = \text{despread}(\tilde{\mathbf{X}}/\mathbf{H})$ 
2   $\beta, \epsilon = \text{computeErrors}(\tilde{\mathbf{d}})$ 
3   $\alpha = \text{getEstimate}(\beta)$ 
4  if  $\epsilon < \epsilon_{good}$  or  $\epsilon > \epsilon_{last}$ 
5      return  $\alpha, \epsilon$ 
6   $\alpha'_1, \epsilon'_1 = \text{EQUALIZE}(\tilde{\mathbf{X}}, \mathbf{H}e^{j\alpha}, \epsilon)$ 
7   $\alpha'_2, \epsilon'_2 = \text{EQUALIZE}(\tilde{\mathbf{X}}, \mathbf{H}e^{-j\alpha}, \epsilon)$ 
8  if  $\epsilon'_1 < \epsilon'_2$ 
9      return  $\alpha'_1, \epsilon'_1$ 
10 else
11     return  $\alpha'_2, \epsilon'_2$ 

```

3) *Discussion and Trade-offs:* Equalization techniques that use feedback from the data itself to correct channel are usually referred as blind-equalization [33], [34]. The advantage of this technique is that the receiver does not need the training samples or pilots to estimate the channel but instead take advantage on the larger information of received data and iterate over it to derive the best estimation. This approach not only provides better channel estimation compared to the traditional approach with pilots in many scenarios, but also enables the flexibility in the design, as it solely bases on the data, and removes the overhead signal for more efficient spectrum usage. On the contrary, by iterating over the data multiple times, the computation cost increases significantly.

IV. SYSTEM IMPLEMENTATION AND EVALUATION

In this section, we briefly introduce our implementation and highlight our system capabilities. Then we provide details on the evaluation of our pilotless channel estimation and equalization. The rest of our system evaluation focuses on spectral efficiency and the possibility for coexistence with other wireless networks such as Wi-Fi.

A. Sprite Pilotless FS-FBMC Implementation

Our Sprite-FBMC system was built as our solution for the SC2 competition, which required, among others, mechanisms for system control on channel switching, signal bandwidth resizing to fit in spectrum pockets, collaborating with other peers and spectrum occupancy prediction using machine learning. Thus, our system is a comprehensive multilayer system that accommodates all aforementioned requirements. For the scope of this paper, we will describe only the main components of our physical layer.

Our system implementation is modular, providing flexibility to configure the type of multicarrier technique (FBMC or OFDM), the equalization technique (pilot-based or pilotless) and signal bandwidth (via sample rate or selecting the number of subcarriers).

As FS-FBMC introduces an overhead in computational complexity due to the use of a K times larger FFT, optimization plays an important role in our implementation to reduce system latency to an acceptable level for real-time scenarios (e.g., VoIP traffic). To support real-time processing, along with the use of FFTW [35] and VOLK [36] libraries that perform single-instruction-multiple-data (SIMD) processing for computation optimization, we implemented our system to feature multi-threading for transmitting and receiving simultaneously. By using one or multiple threads for scanning incoming signals, and spawning another new processing thread for each detected packet, a receiver can handle multiple transmissions from multiple transmitters at the same time. Moreover, apart from being able to operate in real-time by streaming from and to SDRs, our system is also able to operate with a file as input/output for reproducibility of results.

Our system can operate flexibly with different parameters for FBMC modulation. In particular, with overlapping factor $K = 4$, the number of subcarriers N can vary from 64 to 256, which makes the signal bandwidth flexible in a wide range from 156 kHz to 20 MHz with steps as small as 156 kHz for a fixed sample rate of 20 MHz. By using different combinations of these parameters, our system can shrink the signal to a small spectrum pocket when the channel is crowded or stretch to operate over a wider bandwidth.

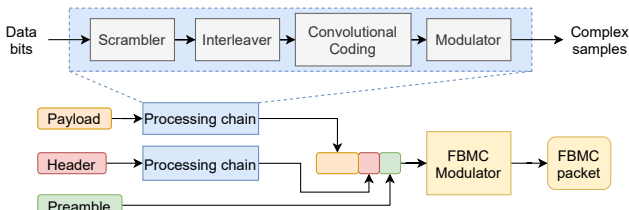


Fig. 7: Block diagram of FBMC packet creation, including preamble, header and payload data generated from the network layer.

As a full-stack network system, we support multi-rate via modulation and coding schemes that can be specified in each packet. Our FBMC packets consist of preamble, header and payload constructed through separated chains as shown in Figure 7. The preamble is a known sequence defined in frequency domain to support packet detection and frame synchronization. The header contains payload information including its length and modulation coding scheme. Both header and payload are generated separately following the steps in the processing chain in Figure 7. Data bits are first scrambled for sequence whitening, and then interleaved before passing through the convolutional coding and modulator block for the desired rate. The header and payload modulated symbols along with preamble are finally input to the FBMC modulator to construct the FBMC packet.

B. Experimental Setup

We evaluate our system through two different setups with different level of approximation to a real world scenario.

Scenario A: The first setup aims at evaluating our system isolated from effects of hardware and other impairments. To

do so, we use the transmitter to generate FBMC complex signals from an input binary data, and we feed the complex signals to a simulated channel to undergo the channel effects. The received signal is input to our FBMC receiver which performs the necessary steps to decode the original data from signal detection, channel estimation and equalization to data decoding. The channel simulation block is performed using MATLAB software. We import the FBMC complex symbols output by the transmitter into MATLAB and add the effects of AWGN channel model with different SNR values.

Scenario B: To include an additional layer of realism and complexity to our test environment, we carry out the experiment on Colosseum [37], a large RF emulator designed to support research and development of large-scale radio networks. We configure our experiments in a Line-Of-Sight environment where multiple nodes form pairs of transmitter-receiver and operate over the same band. The transceivers use USRP X310 SDRs to transmit and receive the IQ signals, which pass through an emulated channel to the receiver. For this scenario, we aim to compare the spectrum efficiency and flexibility of our FBMC system and those of an OFDM-based system. For the OFDM-based transceiver, we use SWiFi [38], an open source Wi-Fi implementation for SDRs.

In both setups, we configure FBMC parameters with overlapping factor $K = 4$ and total number of subcarriers $N = 256$, corresponding to a 20 MHz operative bandwidth. Although our system can operate over wide bandwidths, we select a subset of $n = 22$ consecutive subcarriers for most scenarios, unless otherwise stated. This is equivalent to 1.7 MHz, which matches better typical scenarios for opportunistic and cognitive radios.

C. Pilotless Equalization Performance

In this section, we evaluate our equalization technique by analyzing its performance under different noise levels and physical layer configurations. We carry out our experiments in Scenario A. The transmitter generates 10000 packets, each of 1000 bytes, which pass through the channel at different SNR values. The Bit-Error-Rate (BER) is computed at the receiver during the packet reception by comparing the decoded data that was input to the transmitter.

1) *Performance over different modulation schemes:* As a basic evaluation, we run the pilotless equalization with different modulation schemes at various SNR levels. We compare the following schemes: 16-QAM and 64-QAM (uncoded), and 16-QAM 3/4, 64-QAM 3/4. Figure 8 shows the BER as a function of the SNR in dB for the aforementioned modulations. Results show that our system can achieve a BER as low as 10^{-6} between 12 dB to 21 dB for the modulations under study. 16-QAM is able to reach a BER of 10^{-6} at 15 dB, whereas 64-QAM requires 21 dB to achieve the same figure. The coding scheme improves the modulations by 3 dB and 6 dB for 16-QAM and 64-QAM respectively. Note that at low SNR when the coding fails, the coded scheme can lead some erroneous bits to become more incorrect bits, whereas uncoded communications will have only the error bits due to

the channel, explaining the higher BER of the coded scheme for very low SNR (e.g., 16-QAM 3/4 vs. 16-QAM uncoded at SNR below 8 dB).

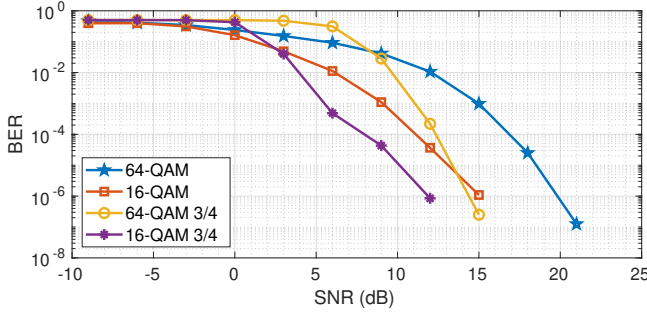


Fig. 8: Bit Error Rate as a function of SNR for our pilotless system when different modulation and coding schemes are used.

2) *Performance with different number of subcarriers used for channel estimation:* Our pilotless equalization is generally performed over all data subcarriers to improve the estimation and cover the channel effect across the complete operating bandwidth. In this subsection we evaluate the channel compensation capabilities when we perform the equalization over a subset of data subcarriers. This can be specially interesting to reduce computation cost as a trade-off with channel estimation required accuracy, for instance, in linear dispersive channels. Figure 9 depicts the BER curves as a function of the SNR for

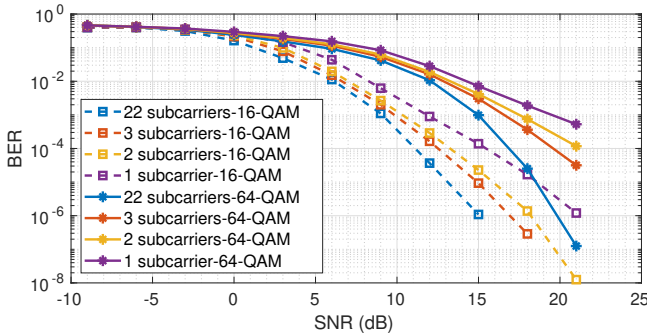


Fig. 9: Comparison of Bit Error Rate as a function of SNR for our pilotless system when variable number of subcarriers are employed for channel estimation.

different number of data subcarriers used in channel estimation for 16-QAM and 64-QAM. We explore the impact of using all (22) versus 3, 2, or only 1 subcarriers used for channel estimation and equalization, which corresponds to using only 13.6%, 9% and 4.5% of available data for our estimation respectively. Results indicate that the equalization performance is considerably degraded by using a subset of subcarriers for estimation, specially for the high-SNR range. The performance degradation is more accentuated for 64-QAM than 16-QAM, and results show that using 3, 2 or 1 subcarrier implies a loss between 3 dB to 6 dB for 64-QAM, whereas the loss ranges between 1 dB to 6 dB for 16-QAM. Therefore, it is preferable to use all the (data) subcarriers for channel estimation since

the computational gain from using only a subset of (data) subcarriers is not worth the BER degradation.

3) *Comparison with Pilot-Based System:* In this experiment, we evaluate the impact of relying on unknown data (pilotless) compared to using pilots for our system. With the pilot-based configuration, the receiver has prior knowledge of the original data symbols on a few subcarriers and performs the channel estimation algorithm over only these given pilots. Figure 10 shows the BER achieved by the pilotless and pilot-

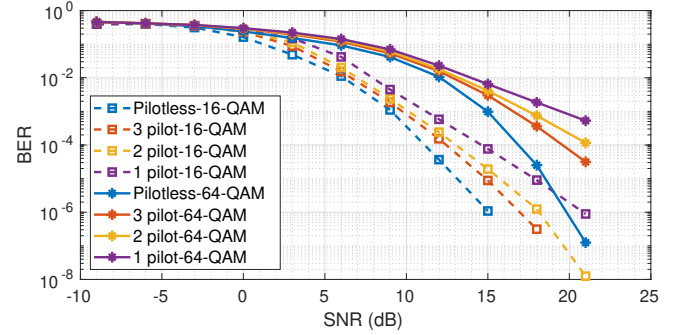


Fig. 10: Comparison of Bit Error Rate as a function of SNR for our pilotless system when a set of subcarriers are used as known values to the receiver (pilots).

based approaches for 16-QAM and 64-QAM. For pilot-based experiment, we configure the system to use 1, 2, or 3 pilot subcarriers. Results show that there is a BER degradation by using a reduced set of pilots. For example, a minimum degradation of 1 dB loss is incurred to the 3-pilot system in comparison to the pilotless system when using 16-QAM modulation. In fact, results are practically identical to the results found in Figure 9, suggesting that our channel estimation and equalization algorithm does not benefit from the use of pilots. As our system does not require any prior knowledge, therefore the spectral efficiency is improved.

D. Spectral Efficiency

Apart from the reduced out-of-band-emissions, another of the key aspects of FBMC is the improvement in spectral efficiency, thanks to the omission of cyclic prefix, compared to CP-OFDM. We evaluate and compare the spectral efficiency of our system with that of an OFDM-based system in a real-time scenario. The experiments are carried out on Colosseum with two different setups, each consisting of a pair of transmitter and receiver. In the first setup, two nodes run our Sprite implementation and are configured to transmit and receive at different signal bandwidths by using different number of subcarriers while keeping the same sampling rate of 20 MHz. This setup represents our spectrum-flexible FBMC system that can transmit and receive a flexible signal in real-time without interrupting the hardware for reconfiguration. In the second setup, we use SWiFi implementation [38] to transmit and receive Wi-Fi signals with different bandwidth by adjusting sampling rate (to match the FS-FBMC bandwidth). In both setups, nodes are configured to use the same modulation-coding scheme 16-QAM 1/2 to send and receive packets

of size 1000 bytes. The transmit and receive gains in both setups are configured to maintain a good SNR of 20 dB at the receivers so that the channel does not impact our study of spectral efficiency.

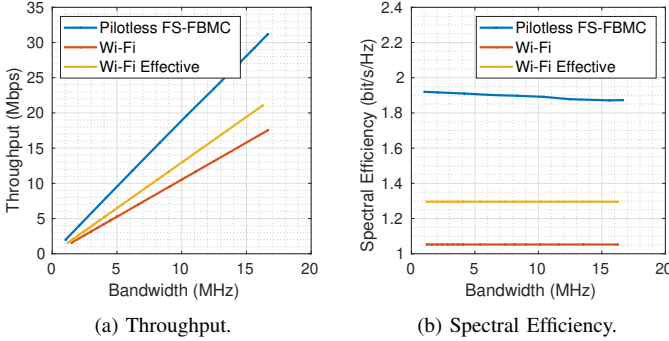


Fig. 11: Throughput and spectral efficiency achieved for 16-QAM 1/2 with spectrum-flexible FBMC and Wi-Fi at different bandwidth.

Figure 11 shows the performance results as a function of the signal bandwidth for FBMC and Wi-Fi (OFDM). Note that the Wi-Fi protocol operates over channels of fixed bandwidth (e.g. 20 MHz) and leaves 5 or 6 null subcarriers (out of a total 64 subcarriers) on each side of the transmission to protect from cross Wi-Fi channel interference. Thus, we take this detail into account and along with the evaluation of Wi-Fi as per the standard, we also derive the performance of Wi-Fi considering only the effective bandwidth (shown as Wi-Fi Effective in Figure 11), which is defined as the total spectrum occupied by the data and pilot subcarriers, excluding null subcarriers. For our FBMC design, thanks to the low interference of the transmission, we only require one null subcarrier at the edges, hence, our FBMC channel and signal bandwidth are almost equivalent.

Figure 11a depicts the achieved throughput by the FBMC and Wi-Fi systems. Results show that our spectrum-flexible FBMC is able to consistently provide a higher throughput, for 16.25 MHz, our FBMC system is able to achieve a throughput of 30.42 Mbps whereas the standard Wi-Fi system can reach 17.5 Mbps and 21.05 Mbps when considering only effective bandwidth. The improvement of FBMC over Wi-Fi is the result of the cyclic prefix removal in FBMC and the absence of pilots, which boosts spectral efficiency.

To have a better quantification, we compute the spectral efficiency by normalizing the throughput to a spectrum unit, i.e., bit rate per Hertz (bit/s/Hz), for each signal bandwidth. Figure 11b shows the spectral efficiency of our FBMC design and Wi-Fi. It can be seen that FBMC spectral efficiency is about 1.9 bit/s/Hz, making a great improvement of 80% over Wi-Fi's, which is at 1.05 bit/s/Hz. As for Wi-Fi effective bandwidth, since null subcarriers are not considered for the computation, its spectral efficiency increases to 1.3 bit/s/Hz, a value that our FBMC system still improves by 46%. We note that the slight decrease of FBMC's spectral efficiency as bandwidth increases is due to the tail of the last FBMC symbol consisting of $(K - 1/2)N$ samples that do not overlap with

preceding FBMC symbols. This tail effect is a well known overhead of FBMC modulation that makes it less efficient for short bursts. However, it is almost negligible for long packets, such as 1000 bytes, where FBMC significantly outperforms Wi-Fi OFDM as observed from the results.

E. Spectrum Flexibility & Wi-Fi Coexistence

Due to our flexible design, our system can easily fit in any spectrum gap that is available simply by selecting different subbands for transmissions. To highlight the flexibility and low out-of-band emissions, we consider a crowded scenario where two non-overlapping 20 MHz Wi-Fi channels are continuously transmitting. Wi-Fi protocol requires a spacing of 25 MHz between the two center frequencies of these channels to prevent interference, this leaves an empty gap of 5 MHz. Ideally in this situation, the gap would be filled by a narrow bandwidth signal that does not interfere with the Wi-Fi channels, boosting the total aggregated capacity of the channel. Our system can achieve this goal efficiently and effectively. Figure 12 shows the spectrum view of this scenario, where our FBMC signal fits in between the gap of two Wi-Fi channels. Analogously to the spectral efficiency experiment, we configure the transmit and receive gains on each pair of nodes to maintain the same SNR of 20 dB at the receivers, ensuring the fairness in our interference analysis.

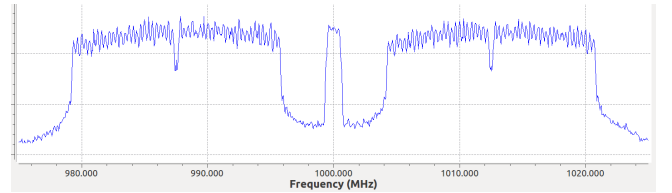


Fig. 12: A realtime spectrum view shows a spectrum-flexible FBMC transmission fit in between two non-overlapping Wi-Fi channels.

Now since our system can have flexible transmissions, we vary our signal bandwidth to analyze the impact of system on Wi-Fi transmissions. To do so, we introduce the Packet Reception Ratio (PRR) metric, defined as the ratio of the number of packets received correctly and the total number of received packets. Figure 13 shows the PRR achieved for each communication link when our system is transmitting in the gap between two non-overlapping Wi-Fi channels. Note that the Wi-Fi spacing and guard band are only 5 MHz in total, our transmission actually overlaps with the 20 MHz region of Wi-Fi signal without interfering. The critical point of interference in this scenario is achieved when the FBMC signal bandwidth reaches 8.125 MHz. Beyond this point, the performance of all transmissions starts to drop sharply, and all communication links become disconnected within a 2 MHz increase. This is because although Wi-Fi signal has a bandwidth of 20 MHz, the actual bandwidth used for data and pilot is only 16.25 MHz and the rest is reserved as a prevention for the leakage to adjacent channels. The PRRs achieved with FBMC signal bandwidth up to 8.125 MHz indicates that our system introduces a very low interference to neighboring Wi-Fi channels

while maintaining its performance under Wi-Fi interfering leakages. The discrepancies in the PRR results between the two Wi-Fi signals is explained by the fact that Wi-Fi leaves 5 empty subcarriers on the left, and 6 empty subcarriers in the right as guard bands. Hence, due to the slightly wider gap in the right (312.5 kHz), the Wi-Fi link on the right channel is less impacted by interference.

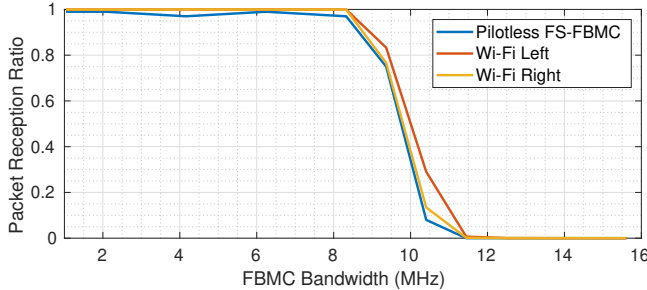


Fig. 13: FBMC coexistence with two fixed 20 MHz Wi-Fi channels spaced by 5 MHz shows up to 8.125 MHz of FBMC channel can fit in between without causing packet reception ratio degradation.

V. CONCLUSION

We introduce a set of techniques and design for a pilotless spectrum-flexible FS-FBMC. Our design, algorithms, and techniques are implemented in a full network stack and extensively evaluated for its performance. We demonstrate flexibility (as low as 156 kHz), robustness, and 46% better spectral efficiency relatively to OFDM-CP (Wi-Fi). We also show co-existence with Wi-Fi including operation in narrow pockets of spectrum between Wi-Fi signals.

REFERENCES

- [1] Federal Communications Commission, "Cognitive Radio for Public Safety," <https://www.fcc.gov/general/cognitive-radio-public-safety>.
- [2] Samsung, "Dynamic Spectrum Sharing. Technical White Paper," 2021.
- [3] W. S. H. M. W. Ahmad, N. A. M. Radzi, F. S. Samidi, A. Ismail, F. Abdullah, M. Z. Jamaludin, and M. N. Zakaria, "5G Technology: Towards Dynamic Spectrum Sharing Using Cognitive Radio Networks," *IEEE Access*, 2020.
- [4] S. Haykin, "Cognitive radio: brain-empowered wireless communications," *IEEE Journal on Selected Areas in Communications*, 2005.
- [5] DARPA, "Spectrum Collaboration Challenge (SC2)," <https://www.darpa.mil/news-events/2018-12-19>, <https://www.darpa.mil/news-events/2019-09-10>.
- [6] R. W. Chang, "Synthesis of band-limited orthogonal signals for multi-channel data transmission," *The Bell System Technical Journal*, 1966.
- [7] B. Saltzberg, "Performance of an Efficient Parallel Data Transmission System," *IEEE Transactions on Communication Technology*, 1967.
- [8] A. Viholainen, T. Ihalainen, T. H. Stütz, M. Renfors, and M. Bellanger, "Prototype filter design for filter bank based multicarrier transmission," in *2009 17th European Signal Processing Conference*, 2009.
- [9] V. Berg, J.-B. Doré, and D. Noguét, "A Multiuser FBMC Receiver Implementation for Asynchronous Frequency Division Multiple Access," in *2014 17th Euromicro Conference on Digital System Design*, 2014.
- [10] B. Farhang-Boroujeny, "OFDM Versus Filter Bank Multicarrier," *IEEE Signal Processing Magazine*, 2011.
- [11] F. Schaich, J. Vandermot, V. Ringset, H. Rustad, M. Najjar, F. Rubio, M. Caus, and Z. Zhipeng, "WiMAX simulation results – Lab setup and measurements", PHYDYAS Deliverable D9.3."
- [12] H. Bölcskei, *Orthogonal Frequency Division Multiplexing Based on Offset QAM*. Birkhäuser Boston. Advances in Gabor Analysis, 2003.

- [13] P. Siohan, C. Siclet, and N. Lacaille, "Analysis and design of OFDM/OQAM systems based on filterbank theory," *IEEE Transactions on Signal Processing*, 2002.
- [14] A. I. Pérez-Neira, M. Caus, R. Zakaria, D. Le Ruyet, E. Kofidis, M. Haardt, X. Mestre, and Y. Cheng, "MIMO Signal Processing in Offset-QAM Based Filter Bank Multicarrier Systems," *IEEE Transactions on Signal Processing*, 2016.
- [15] R. Zakaria and D. Le Ruyet, "A Novel Filter-Bank Multicarrier Scheme to Mitigate the Intrinsic Interference: Application to MIMO Systems," *IEEE Transactions on Wireless Communications*, 2012.
- [16] B. Hirosaki, "An Orthogonally Multiplexed QAM System Using the Discrete Fourier Transform," *IEEE Trans. on Communications*, 1981.
- [17] J. Nadal, C. Abdel Nour, and A. Baghdadi, "Low-complexity pipelined architecture for FBMC/OQAM transmitter," *IEEE Transactions on Circuits and Systems II: Express Briefs*, 2015.
- [18] "PHYDYAS: physical layer for dynamic spectrum access and cognitive radio, European FP7 Project," <http://www.ict-phydyas.org/>.
- [19] "METIS 2020 FP7 Project," <https://metis2020.com/>.
- [20] M. Bellanger, "FS-FBMC: An alternative scheme for filter bank based multicarrier transmission," in *2012 5th International Symposium on Communications, Control and Signal Processing*, 2012.
- [21] M. Bellanger, D. LeRuyet, D. Roviras, M. Terré, J. Nossek *et al.*, "FBMC physical layer: a primer," in *PHYDYAS*, 2010.
- [22] J. Nadal, C. A. Nour, and A. Baghdadi, "Design and Evaluation of a Novel Short Prototype Filter for FBMC/OQAM Modulation," *IEEE Access*, 2018.
- [23] J.-P. Javaudin, D. Lacroix, and A. Rouxel, "Pilot-aided channel estimation for OFDM/OQAM," in *The 57th IEEE Semiannual Vehicular Technology Conference, 2003. VTC 2003-Spring.*, 2003.
- [24] C. Lele, R. Legouable, and P. Siohan, "Channel estimation with scattered pilots in OFDM/OQAM," in *2008 IEEE 9th Workshop on Signal Processing Advances in Wireless Communications*, 2008.
- [25] C. Lele, P. Siohan, R. Legouable, and J.-P. Javaudin, "Preamble-based channel estimation techniques for OFDM/OQAM over the powerline," in *IEEE International Symposium on PLC and Its Applications*, 2007.
- [26] W. Cui, D. Qu, T. Jiang, and B. Farhang-Boroujeny, "Coded Auxiliary Pilots for Channel Estimation in FBMC-OQAM Systems," *IEEE Transactions on Vehicular Technology*, 2016.
- [27] Z. Zhao, N. Vucic, and M. Schellmann, "A simplified scattered pilot for FBMC/OQAM in highly frequency selective channels," in *11th International Symposium on Wireless Communications Systems*, 2014.
- [28] M. Fuhrwerk, S. Moghaddamia, and J. Peissig, "Scattered Pilot-Based Channel Estimation for Channel Adaptive FBMC-OQAM Systems," *IEEE Transactions on Wireless Communications*, 2017.
- [29] Y. Won, J. Oh, J. Lee, and J. Kim, "A Study of an Iterative Channel Estimation Scheme of FS-FBMC System," *Wireless Communications and Mobile Computing*, 2017.
- [30] J. Ketonen, M. Juntti, and J. Ylioinas, "Decision directed channel estimation for improving performance in LTE-A," in *Conference Record of the 44th Asilomar Conf. on Signals, Systems and Computers*, 2010.
- [31] J. Ran, R. Grunheid, H. Rohling, E. Bolinoh, and R. Kern, "Decision-directed channel estimation method for OFDM systems with high velocities," in *57th IEEE Semiannual Vehicular Technology Conf.*, 2003.
- [32] A. W. Azim, Y. Le Guennec, and G. Maury, "Decision-directed iterative methods for PAPR reduction in optical wireless OFDM systems," *Optics Communications*, 2017.
- [33] G. Picchi and G. Prati, "Blind Equalization and Carrier Recovery Using a "Stop-and-Go" Decision-Directed Algorithm," *IEEE Transactions on Communications*, 1987.
- [34] C. Fernandes, G. Favier, and j. Mota, "Decision directed adaptive blind equalization based on the constant modulus algorithm," *Signal, Image and Video Processing*, 2007.
- [35] M. Frigo and S. Johnson, "The Design and Implementation of FFTW3," *Proceedings of the IEEE*, 2005.
- [36] "Vector-Optimized Library of Kernels," <https://www.libvolk.org>.
- [37] Colosseum Team, "Colosseum The World's Most Powerful Wireless Network Emulator," <https://www.northeastern.edu/colosseum>.
- [38] T. D. Vo-Huu, T. D. Vo-Huu, and G. Noubir, "SWiFi: An Open Source SDR for Wi-Fi Networks High Order Modulation Analysis," Northeastern University, Tech. Rep., 2015.